Electrostatic Force Theory for a Molecule and Interacting Molecules. 7. Ab Initio Verification of the Force Concepts Based on the Floating Wave Functions of NH_3, CH_3^+, and NH_3^+

H. Nakatsuji,* S. Kanayama, S. Harada, and T. Yonezawa

Contribution from the Department of Hydrocarbon Chemistry, Faculty of Engineering, Kyoto University, Kyoto, Japan. *Received May 1, 1978*

Abstract: We have reexamined the concepts of the electrostatic force (ESF) theory applied to molecular geometry, using the ab initio wave functions which satisfy the Hellmann–Feynman theorem. The floating wave functions, in which the centers of all the AOs (here, minimal STO-3G basis) were floated and determined variationally, were calculated for the AH_3 molecules, NH_3, CH_3^+, and NH_3^+. We have elucidated the origins of the molecular shapes from the analyses of the forces F_A and F_H and the density behaviors. They are shown to be in good parallelism with the ESF pictures developed previously. The utilities of the pictures of F_A and F_H are also compared briefly.

Force concept based on the Hellmann–Feynman (H–F) theorem[1] has provided a useful theoretical viewpoint for the studies of various nuclear rearrangement processes.[2] In the previous papers of this series,[3,4] we have shown that molecular geometries are easily understood and predicted by the electrostatic force (ESF) theory. Similar concepts have also been applied to some typical systems of chemical reactions[5,6] and long-range forces.[3b] On the other hand, Deb has developed a simple mechanical model of molecular geometry based on a HOMO (highest occupied molecular orbital) postulate.[7] A review of various models of molecular geometry has been given in ref 4.

A purpose of this paper is to reexamine the ESF concept of molecular geometry using the ab initio wave functions which satisfy the H–F theorem. Though the success of the ESF theory for molecular geometry may be considered as a proof for the validity of the underlying concept, it is still *inductive* and a more direct proof may be hoped. For instance, some criticisms[8] on the valence-shell electron-pair repulsion theory[9] seem to indicate an existence of the case that general agreements with experiments do not constitute a sufficient condition for the validity of the underlying concept.[4] Here, we have calculated, for this purpose, the floating wave functions[10,11] since they rigorously satisfy the H–F theorem. The AH_3 molecules, NH_3, CH_3^+, and NH_3^+, have been chosen because their shapes were of central importance in the construction of the ESF theory.[3,12] We have elucidated the force and density origins of the molecular shapes and compared them with the previously developed ESF concepts.

Calculation of Floating Wave Function

Hurley[10] has shown that a reason why most of the existing wave functions[13] do not satisfy the H–F theorem is that they are not fully variational since the centers of the AOs (or the bases) are not determined variationally but are fixed on the constituent nuclei. In the fixed AO approximation, the electronic coordinates are not treated as the variables free from the nuclear coordinates, so long as the basis set is incomplete. In order that the H–F theorem is satisfied for the force F_A, it is sufficient that only the AOs belonging to an atom A are floated and their centers are determined variationally.[11] In the present calculations we have floated all of the AOs involved, so that the present wave functions satisfy the H–F theorem for all the forces.

Denote the centers of the AOs $\{\chi_r\}$ as $\{\mathbf{x}_r\}$; then the variational principle requires

$$\frac{\partial}{\partial \mathbf{x}_r}\mathcal{E}(\mathbf{R}_A, \mathbf{x}_r) = 0 \tag{1}$$

where $\mathcal{E}$ is an energy of a trial wave function $\tilde{\Psi}$, $\mathcal{E}(\mathbf{R}_A, \mathbf{x}_r) = \langle \tilde{\Psi}(\mathbf{x}_r)|H(\mathbf{R}_A)|\tilde{\Psi}(\mathbf{x}_r)\rangle$, and $\{\mathbf{R}_A\}$ are the nuclear coordinates. For the present purpose the variational parameters other than $\{\mathbf{x}_r\}$ can be omitted.[11a] The force (or energy gradient) $\mathbf{F}_A$ associated with the trial function $\tilde{\Psi}$ is calculated as

$$\mathbf{F}_A = -\left\langle \tilde{\Psi}\left|\frac{\partial H}{\partial \mathbf{R}_A}\right|\tilde{\Psi}\right\rangle - \sum_r \frac{\partial \mathcal{E}}{\partial \mathbf{x}_r}\frac{\partial \mathbf{x}_r}{\partial \mathbf{R}_A} \tag{2}$$

where the first term represents the H–F force and the second term, which is $-2\langle\tilde{\Psi}|H|\partial\tilde{\Psi}/\partial\mathbf{R}_A\rangle$, is denoted as the error term since it arises *entirely* from the errors included in the wave function. Under the variational condition given by eq 1, the error term vanishes identically and the H–F theorem is satisfied.

$$\mathbf{F}_A = Z_A\{\int \rho(\mathbf{r}_1)\,\mathbf{r}_{A1}/r_{A1}^3\,d\mathbf{r}_1 - \sum_{B(\neq A)} Z_B\mathbf{R}_{AB}/R_{AB}^3\} \tag{3}$$

In the present calculations, the optimal centers of the floating AOs (FAOs) are calculated by the direct procedure proposed by Moccia et al.,[14] though their emphasis has been placed on the optimization of atomic orbital exponents. We have calculated explicitly the term on the left-hand side of eq 1, which may be called "AO force" from an analogy to $\mathbf{F}_A$, and floated all of the AOs simultaneously so as to make all the AO forces vanish identically. This method was more efficient than the previous one.[11] For the Hartree–Fock method of closed-shell systems, which is used for NH_3 and CH_3^+, the AO force acting on χ_r is given by

$$\frac{\partial \mathcal{E}}{\partial \mathbf{x}_r} = \sum_s P_{rs}\Big[2(r'|h|s) + \sum_{t,u} P_{tu}\{2(r's|tu) - (r't|su)\}\Big] - 2\sum_s D_{rs}(r'|s) \tag{4}$$

where r' denotes $\partial\chi_r/\partial\mathbf{x}_r$ and D_{rs} is given by

$$D_{rs} = 2\sum_i^{occ} \epsilon_i C_{ri}C_{si} \tag{5}$$

and the other terms are given in the usual notations.[14,15] Similar equations are also obtained for the unrestricted Hartree–Fock (UHF) method used for NH_3^+. The entire program is similar to that used for the so-called energy gradient calculations.[15] Note, however, that though the so-called energy gradient includes a large contribution from the error term, the present force does not.

Results

The floating wave functions of AH_3 were calculated at several out of plane angles θ (see Figure 1). We have used the

0002-7863/78/1500-7528$01.00/0

minimal STO-3G basis[16] with the standard exponents.[17] The bond lengths were fixed to the values reported by Lathan et al.[18] They are 1.033 Å for NH_3, 1.120 Å for CH_3^+ and 1.056 Å for NH_3^+. The experimental length of NH_3 is 1.012 Å.[18] All of the AOs were floated within the freedom allowed by the symmetry and their optimal positions were determined by making all of the AO forces vanish simultaneously.

In Figure 1, we have plotted the optimal centers of the FAOs as functions of the angles θ. The floating distances of the inner $1s_A$ AOs were very small,[19] as expected, so that they are given in the figure caption. In NH_3, all of the AOs float into the inside of the pyramid. The same is true for NH_3^+ except for the $2p_z$ and inner $1s_N$ AOs. On the other hand, in CH_3^+, all of the AOs float out of the pyramid except for the $2p_x$ and $2p_y$ AOs. Further, for CH_3^+, the position of the $2p_z$ AO seems to diverge at very small angles. This behavior may be understood from the fact that at $\theta = 0°$, the $2p_z$ AO is completely vacant.

In Figure 2, we have plotted the force acting on the central nucleus A, F_A, of the AH_3 molecules, NH_3, CH_3^+, and NH_3^+, against the bending angle θ. In Figure 3, we have plotted the transverse force acting on the terminal proton, $F_{H\perp}$. The SCF energy is given by the dotted line. Since the present wave functions satisfy the H-F theorem for both forces F_A and F_H, the equilibrium angles calculated from the SCF energy, the force F_A, and the force $F_{H\perp}$ are completely the same. The same should be true for all the force-dependent properties. In Table I, we have summarized the equilibrium angles and bending force constants. The present floating results are compared with the results of the fixed AO approximation (with the same basis) and with the experimental (or other theoretical) values. The shapes of NH_3, CH_3^+, and NH_3^+ are calculated to be pyramidal, planar, and planar, respectively, in agreement with other studies. In the present calculations, the effects of the floating are relatively large in contrast to the previous ones in which only the $1s_H$ AOs were floated.[11,20] The reason is seen from Table II, which shows the energy lowering obtained by the floating procedure. It increases rapidly with the increase in the bending angle θ. A large dependence on θ is due to the floating behaviors of the AOs belonging to the central atom A (see Figure 1): at $\theta = 0°$, these FAOs are just on the nucleus A from the symmetry. They float apart from the nucleus A with the increase in the bending angle. Thus, the calculated equilibrium angle, θ_{eq}, of NH_3 is larger in the present calculations than in the fixed AO calculations. Though the calculated angle of NH_3 departs from the experimental value since the value of the fixed AO approximation is already larger than the experimental value,[21] the bending force constants become closer, by floating, to the experimental values. For the bond lengths, however, the effects of floating were negligibly small. In the Appendix, we have shown the effects of floating on the H-F forces and the electron densities.

Force and Density Origins of Molecular Shape

In this section, we elucidate the force and density origins of the shapes of the AH_3 molecules and compare them with the previous ESF concepts. As seen from Figures 2 and 3, the shapes can be studied equivalently from either of the forces F_A and $F_{H\perp}$, or from a linear combination of both. The difference lies only in the choice of the coordinates.[22] Here, we first study the origins of F_A and then the origins of $F_{H\perp}$. Since the pictures of the origins of F_A and $H_{H\perp}$ are different, it is interesting to compare the utilities of the different pictures. Previously, we have used in most cases the force F_A,[3,4] but Deb and his co-workers[7,22] have preferred the use of $F_{H\perp}$.

We partition the H-F force into atomic dipole (AD), exchange (EC), and extended gross charge (EGC) forces.[3a] The pictures of these forces were given in ref 3a and 4. Though the basis AOs were floated here, the definition of the partitioning was not altered from that used for nonfloating wave functions.[23] It might be considered as a modification of the one given earlier by Bader et al.[24]

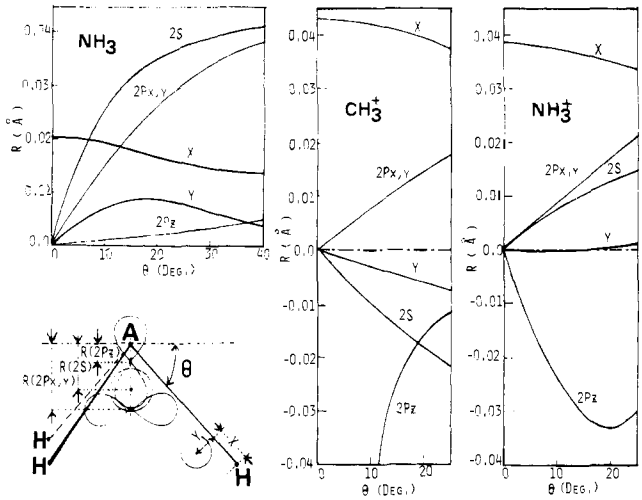

Figure 1. Optimal centers of the floating AOs as functions of the bending angle θ. The distances ($R \times 10^4$ Å) of the inner $1s_A$ AOs are 0.905 (8°), 1.427 (15°), 1.750 (27.2°), 1.704 (40°) for NH_3, −0.742 (10°), −1.033 (15°), −1.602 (24.3°) for CH_3^+, and −0.056 (10°), −0.106 (15°), −0.234 (24.3°) for NH_3^+.

Force Origin of F_A. Figure 2 shows the analysis of the force F_A. As the molecule is bent, the AD force is induced on the nucleus A. It is mainly due to the generation of the lone pair lobe on the atom A. It works to bend the molecule further. It is large in NH_3, median in NH_3^+, and small in CH_3^+, according to the number of the electrons occupied in the lone-pair orbital. The EC(A-H) force represents the attractive force acting on A due to the density in the A-H overlap region. It works to restore the molecule to the planar form since the vector sum of the three EC(A-H) forces along the bonds directs downwards. The EGC(A-H) force represents the force on A due to the nuclear charge of H shielded by the electron density surrounding it. It is repulsive and works to bend the molecule further, since for the present molecules the net gross charge on H is positive (especially for CH_3^+ and NH_3^+). Previously, we have assumed this contribution to be small,[3a] but this assumption is incorrect. However, since both of the EC(A-H) and EGC(A-H) forces are assigned to the A-H bond, it is convenient to define the contribution of the A-H bond by the sum of these two forces, i.e.,

$$\text{bond(A-H) force} = \text{EC(A-H) force} + \text{EGC(A-H) force} \quad (6)$$

As seen from Figure 2, the behaviors and roles of the bond(A-H) forces are determined by those of the EC(A-H) forces even in the positively charged molecules. Namely, the bond(A-H) force pulls the nucleus A along the bond and works to restore the molecule to the planar form. Thus, *the force acting on A, F_A, is understood quantitatively as a sum of the two opposite factors, the AD force and the bond force.*

The analysis given in Figure 2 shows the origins of the molecular shapes as follows. As the NH_3 molecule is bent from the planar form, the AD force is generated very rapidly on N (reflecting the similar behavior of the lone pair density shown in Figure 5), so that it overcomes the contribution of the bond force. Then, the NH_3 becomes pyramidal. Near the equilibrium angle, the AD force ceases to increase since the expansion of the lone pair lobe terminates near this angle (see Figure 5). Therefore, the bond force exceeds the AD force in the angles $\theta > \theta_{eq}$ and restores the molecule again to the equilibrium angle. In CH_3^+, the AD force is very small and the bond force always pulls C downwards. Therefore, the shapes of CH_3^+ is planar. Actually, the total force curve shown in Figure 3 is

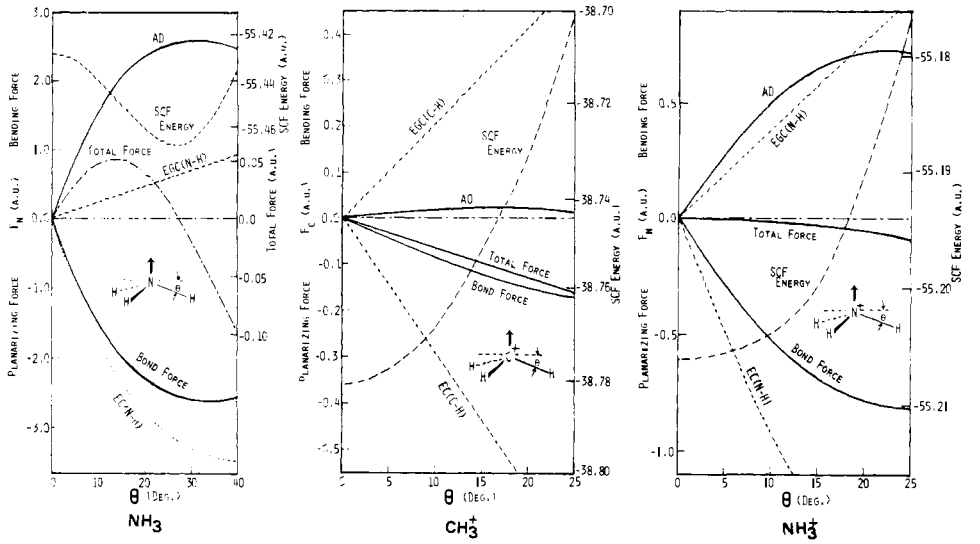

Figure 2. The force acting on the central nucleus A, F_A, of the AH_3 molecule, NH_3, CH_3^+, and NH_3^+, against the out of plane bending angle θ. The SCF energy curves are also given.

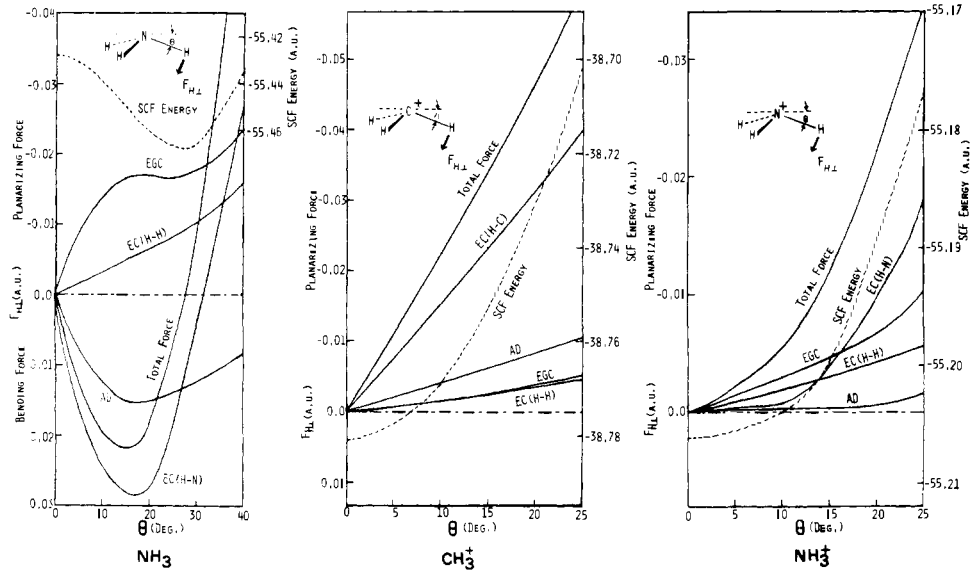

Figure 3. The transverse force acting on the terminal proton, $F_{H\perp}$, of the AH_3 molecule, NH_3, CH_3^+, and NH_3^+, against the out of plane bending angle θ. The SCF energy curves are given by the dotted lines.

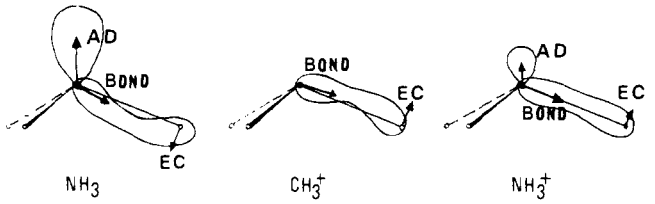

Figure 4. Pictorial summary of the force and density origins of the molecular shapes obtained by the present analysis at $\theta = 15°$.

almost parallel to the curve of the bond force. In NH_3^+, the AD force is median between those of NH_3 and CH_3^+, since its lone pair orbital is singly occupied. Therefore, from the figure of NH_3, the shape of NH_3^+ is expected to be planar. Actually, in Figure 3, the bond force of NH_3^+ exceeds the AD force and leads the molecule to a planar form. In Figure 4, we have given a pictorial summary of the origins of the molecular shape.

Here, we want to note a good parallelism between the above picture of the origins of the molecular shape and the qualitative picture developed in part 1 of this series.[3a] (For instance, Figure 4 may be compared with Figure 6 of part 1.) In part 1, we have used the EC(A-H) force instead of the present bond(A-H) force, assuming that the contribution of the EGC(A-H) force is small. Though this assumption is not correct, it is confirmed here that the behavior of the bond(A-H) force is parallel to that of the EC(A-H) force even for the positively charged species. Therefore, for qualitative purposes, the EC(A-H) force may well be used to understand the behavior of the bond(A-H) force. Thus, the present results may be regarded as giving an ab initio verification of the previous ESF picture used for the AH_3 molecules.

In the above analysis the two opposite factors of F_A, the AD and bond forces, have been assigned to the lone pair and bond, respectively. (See also the density analyses given below.) Since bond and lone pair are the chemical units whose transferability is well established, we may expect a similar transferability for the present force concept. Actually, such an idea seems to be supported by the success in the systematic applications of the ESF theory[3,4] (because if such transferability does not exist, the success could not have been obtained). This point will be examined later with the use of the localized molecular orbitals.[25]

Density Origin. In Figures 5, 6, and 7, we have given the

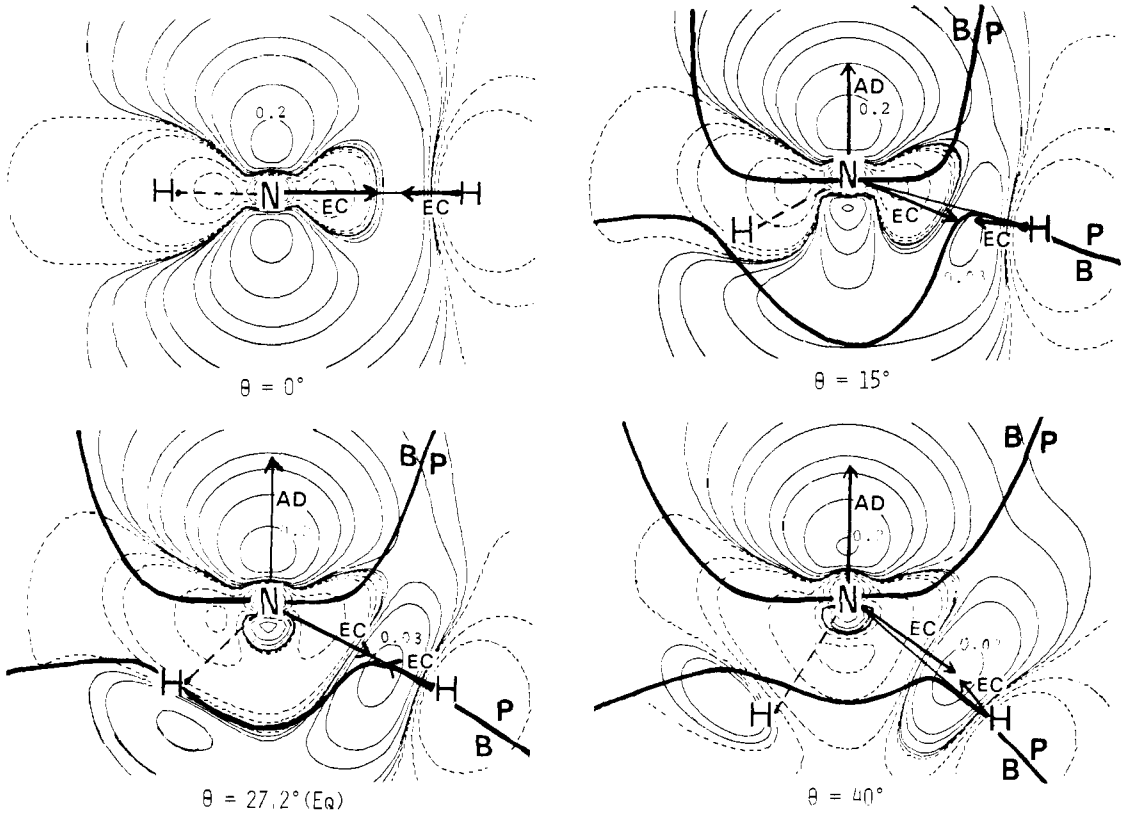

Figure 5. Reorganization of the electron density of NH_3 in the course of the out of plane bending process. Each density difference is defined by eq 7. The real and dotted lines show an increase and decrease, respectively, in the electron density. The solid lines show the generalized Berlin diagram which divides the regions of the electron density into the bending (B) and planarizing (P) regions. The contour values are 0.0, ±0.001, ±0.005, ±0.01, +0.03, ±0.05, ±0.1, and ±0.2.

Table I. Equilibrium Angles and Bending Force Constants Obtained by the Floating Wave Function and by the Fixed AO Approximation

AH_3	equilibrium angle, $\theta_{eq}(\angle HAH)$, deg			bending force constant, mdyn/Å		
	floating[a]	fixed[b,c]	exptl	floating[a]	fixed[b]	exptl
NH_3	27.2 (100.8)	24.3 (104.2)	22.1 (106.7)[c]	0.66	0.80	0.532[f]
CH_3^+	0 (120)	0 (120)	0 (120)[d]	0.97	1.01	0.96[d]
NH_3^+	0 (120)	0 (120)	0 (120)[e]	0.03	0.17	

[a] From the present floating wave functions. [b] From the energies of the fixed AO approximation. [c] Reference 18. [d] Theoretical value: F. Driessler, R. Ahlrichs, V. Staemmler, and W. Kutzelnigg, *Theor. Chim. Acta*, **30**, 315 (1973). [e] T. Cole, *J. Chem. Phys.*, **35**, 1169 (1961). [f] J. L. Duncan and I. M. Mills, *Spectrochim. Acta*, **20**, 523 (1964).

Table II. Energy Lowerings ($\Delta E \times 10^3$) Due to the Floating (au)[a]

AH_3	energy lowerings at various bending angles (θ)						
	0°	8°	10°	15°	24.3°	27.2°	40°
NH_3	2.49	5.86		11.97	19.95	22.09	30.52
CH_3^+	8.79		9.41	9.92	11.34		
NH_3^+	5.95		7.80	9.57	13.37		

[a] $\Delta E = E(\text{nonfloat}) - E(\text{float})$.

density difference maps of NH_3, CH_3^+, and NH_3^+, respectively. They are defined by[26]

$$\Delta\rho(\theta) = \rho_{AH_3}(\theta) - \{\rho_A + \rho_{H_1} + \rho_{H_2} + \rho_{H_3}\} \qquad (7)$$

so that each map shows the change in the density due to the molecular formation from the separated atoms. The real and dotted lines show an increase and decrease in the electron density. The solid lines show the generalized Berlin diagram which divides the regions of the electron density into the bending (B) and planarizing (P) regions.[27] It was drawn with the use of the center of mass of the nuclei (CMN) coordinates. A comparison of the $\Delta\rho(\theta)$ maps at different angles shows the dynamic behavior of the electron density in the bending process. From the density guiding rule,[3c] we expect that the nuclei are pulled in the direction of the electron-cloud reorganization.

In Figure 5, we see that when NH_3 is bent by $\theta = 15°$ from the planar form, the electron density rapidly accumulates over N. This corresponds to a formation of the lone pair lobe on N, and is the origin of the AD force shown by the arrow. The lone pair generates very rapidly at small angles, but ceases to generate at about the equilibrium angle ($\theta = 27.2°$), and at $\theta = 40°$, it rather shrinks as seen from the contour 0.2 au. This behavior is reflected in the similar behavior of the AD force shown in Figure 2. On the other hand, the density in the N–H region pulls N along the bond. At $\theta = 15°$, however, the density is not on the A–H axis (see the contour 0.03 au), but bends inward of the N–H axis. This behavior is the electron-cloud

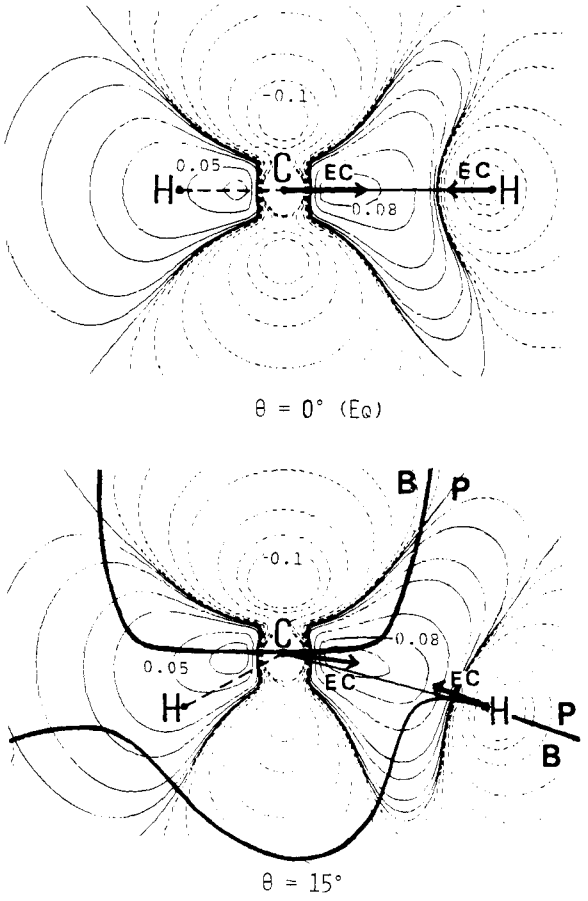

Figure 6. Reorganization of the electron density of CH_3^+ in the course of the bending process. The contour values are 0.0, ±0.001, ±0.003, ±0.01, ±0.02, ±0.05, ±0.08, and ±0.1. Other details are the same as in Figure 5.

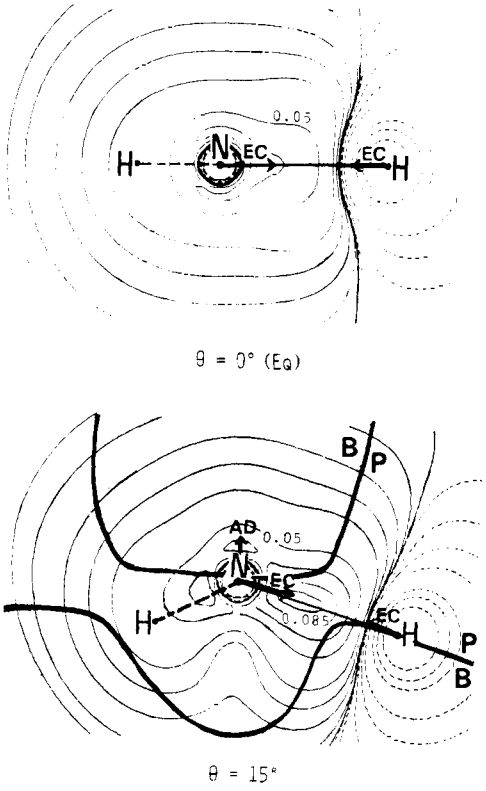

Figure 7. Reorganization of the electron density of NH_3^+ in the course of the bending process. The contour values 0.0, ±0.003, ±0.004, ±0.01, ±0.02, ±0.05, ±0.07, and −0.1 for both $\theta = 0$ and 15° and additionally +0.085 and 0.092 for $\theta = 15°$. Other details are the same as in Figure 5.

preceding since the bond density precedes the bending displacement of the N–H axis. (In other words, the density flows from the P region to the B region.) This bent bond nature is important especially because it induces the EC(H–N) force on the terminal proton in the *bending* direction. At the equilibrium angle, a small bent bond nature is still seen.[28] It works to keep the terminal proton in the electrostatic equilibrium against the interproton repulsions (see Figure 3). However, when the molecule is bent further to $\theta = 40°$, the density in the N–H region cannot follow the bending displacement of the A–H axis (incomplete following). The bond is characterized as the outward bent bond as seen from the arrows of the EC(N–H) and EC(H–N) forces. The latter gives again an important contribution to the transverse force $F_{H\perp}$ (see Figure 3). In Figure 4, we have summarized schematically the behaviors and the roles of the electron density at $\theta = 15°$. At $\theta = 40°$, the behavior of the bond density is just reverse.

Figure 6 shows a similar map of CH_3^+. Since the density behavior was monotonous in CH_3^+, we have given the maps at $\theta = 0$ and 15° alone. At $\theta = 15°$, the density in the atomic region of C flows from the B region to the P region. The density in the C–H region shows a nature of upward bent bond (incomplete following). This is also seen from the directions of the EC(C–H) and EC(H–C) forces shown by the arrows. Thus, from the density guiding rule, the shape of CH_3^+ is expected to be planar. A schematic summary is given in Figure 4.

Figure 7 illustrates the density behavior of NH_3^+. For this molecule, no appreciable changes are induced by the bending. However, we can see a small upward polarization of the density near N, and a small extent of incomplete following in the N–H region as seen from the arrows of the EC forces.

Recently, a development in X-ray measurements has made it possible to observe experimentally the electron density distributions in crystalline molecules.[29] By this technique, the bent bond has been observed for some three-membered ring compounds,[30] as predicted earlier theoretically by Coulson and Moffitt.[31] Here, we predict, on the basis of the generality of the density-guiding rule,[3c] that the bent bond should occur *very frequently* at the geometry *apart* from the equilibrium one. The extent and the direction of the bent bond can be understood from the density-guiding rule.

Force Origin of $F_{H\perp}$. In the previous papers,[11] we have studied the origin of the transverse force, $F_{H\perp}$, of the molecules OH_2, NH_3, and CH_3^+, using the floating wave functions which satisfy the H–F theorem only for the force F_H. The present results are similar to the previous ones, though the numerical results have largely been modified by the additional floating of the AOs of the central atom A. We show here the origins of the force $F_{H\perp}$ only briefly.

In Figure 3, we have shown the analysis of the force $F_{H\perp}$. For NH_3 and CH_3^+, the dominant factor is the EC(H–A) force. It shows a good parallelism to the total force curve. It arises from the bent bond nature of the bond density in the course of the bending process as depicted in Figures 5 and 6. The inward bent bond (i.e., the electron-cloud preceding) of NH_3 at $\theta = 15°$ pulls H in the bending direction, while the upward bent bonds (i.e., incomplete following) of NH_3 at $\theta = 40°$ and of CH_3^+ at $\theta > 0°$ pull H in the reverse direction (see Figure 4). Note that if the bond density is just on the A–H axis (straight bond), its EC(H–A) force does not have a component parallel to the $F_{H\perp}$. The origins of the other minor forces are as follows. The AD force has arisen from the floating of the ls_H AOs of the terminal hydrogens. The 1s density floating apart from the proton pulls it in the direction of floating. The EGC and EC(H–H) forces mainly represent the nonbonded interactions of a proton with the other A–H bonds, so that they are

Table III. Improvement in the H-F Force, F_A, Due to the Floating (au)[a]

AH_3	θ, deg	total H-F force	error	AD	EC(A-H)	EGC(A-H)
NH_3	15	0.052	0.000	2.055	−2.358	0.355
		(1.600)	(1.575)	(3.168)	(−2.001)	(0.433)
	27.2	0.001	0.000	2.570	−3.215	0.645
	(eq)	(2.196)	(2.209)	(4.393)	(−2.926)	(0.729)
	40	−0.098	0.000	2.463	−3.494	0.934
		(2.378)	(2.469)	(4.657)	(−3.273)	(0.994)
CH_3^+	15	−0.099	0.000	0.023	−0.433	0.311
		(−0.358)	(−0.257)	(−0.329)	(−0.398)	(0.369)
NH_3^+	15	−0.032	0.000	0.653	−1.265	0.581
		(0.236)	(0.279)	(0.710)	(−1.118)	(0.644)

[a] Values in parentheses are obtained by the fixed AO approximation. At $\theta = 0°$, all of the values are zero from the symmetry.

Table IV. Improvement in the H-F Force, $F_{H\perp}$, Due to the Floating ($F_{H\perp} \times 10^2$ au)[a]

AH_3	θ, deg	total H-F force	error	AD	EC(H-A)	EC(H-H)	EGC
NH_3	15	2.18	0.00	1.52	2.81	−0.48	−1.66
		(−1.53)	(−2.82)	(0.0)	(1.08)	(−0.45)	(−2.16)
	27.2	0.01	0.00	1.32	1.25	−0.87	−1.69
	(eq)	(−3.72)	(−3.02)	(0.0)	(−0.13)	(−0.92)	(−2.67)
	40	−5.75	0.01	0.85	−2.68	−1.57	−2.35
		(−8.42)	(−2.07)	(0.0)	(−3.33)	(−1.75)	(−3.34)
CH_3^+	15	−3.42	0.00	−0.64	−2.32	−0.23	−0.23
		(−2.95)	(0.58)	(0.0)	(−2.12)	(−0.23)	(−0.61)
NH_3^+	15	−1.19	0.00	−0.03	−0.39	−0.31	−0.46
		(−2.05)	(0.49)	(0.0)	(−0.74)	(−0.29)	(−1.02)

[a] Values in parentheses are obtained by the fixed AO approximation. At $\theta = 0°$, all of the values are zero from the symmetry.

repulsive for all the molecules studied here. We note that the unmonotonous behavior of the EGC force of NH_3 is due to the behavior of the lone pair density on N. It generates rapidly at small angles but ceases to generate at larger angles (see Figure 5).

For NH_3^+, no dominant factor seems to exist at smaller angles. At larger angles ($\theta > 15°$), the EC(H-N) force rapidly increases and becomes the most important factor. Owing to this behavior, a large anharmonicity is expected for NH_3^+, as seen from the SCF energy and total force curves.

Thus, for the force $F_{H\perp}$, the EC(H-A) force, which reflects the bent bond nature of the A-H bond in the course of the bending process, is considered to be a most important factor. As the density-guiding rule implies, the shape of the AH_3 molecule can be predicted from the direction of the bent bond.

Comparison of the Pictures of F_A and $F_{H\perp}$. The shapes of the AH_3 molecules can be studied equivalently from either of the forces F_A and $H_{H\perp}$. However, as seen above, the pictures of F_A and $F_{H\perp}$ are different. The preference depends on the nature of the problem and on the utility of the picture (e.g., an easiness in the understandings and predictions). In this respect, the picture of the force F_A seems to be superior to the picture of the force $F_{H\perp}$, at least for the shapes of the AH_3 and related molecules. Since F_A is composed of only two forces and they are related with the chemically transferable units, lone pair and bond, we can easily extend the picture to other systems in order to understand or predict their shapes. Further, the substituent effects, central atom effect, etc., on these forces have well been established in this series.[3] Examples of such applications are seen in parts 1-3 and in ref 4. On the other hand, for the force $F_{H\perp}$, the number of the factors is larger than for F_A. Though the main factor is shown to be the direction of the bent bond which occurs in the course of the bending process, it is a more detailed property of the density than the bond or lone pair themselves required for F_A. (In an ad hoc manner, however, the direction of the bent bond is easily predicted by the density-guiding rule.) Generally speaking, however, the utility of the different picture depends on the nature of the problem under consideration. For instance, for the problems of internal rotation barrier, the transverse force acting on the terminal nucleus has given a useful picture.[3a,4]

Acknowledgment. One of the authors (H.N.) would like to thank Professor K. Morokuma for some useful discussions. Part of this study has been supported by the Scientific Research Grants from the Ministry of Education.

Appendix. Effects of Floating on the H-F Force and Density

Tables III and IV show the improvements in the H-F forces F_A and $F_{H\perp}$, respectively, obtained by the floating procedure. They clearly show that at this level of basis set, the fixed AO approximation is a very crude approximation in the criterion of the H-F theorem. Though the error term is very large in the fixed AO approximation (see the values in parentheses), it is essentially zero for the present floating wave functions. The largest improvements are seen for NH_3 in both F_A and $F_{H\perp}$. In the forces F_A of NH_3 and CH_3^+ (Table III), the AD force is most improved. This is expected from the natures of the force operator ($\sim r_{Al}/r_{Al}^3$) and the floating procedure. In NH_3^+, the change in the AD force is relatively small. Between the EC(A-H) and EGC(A-H) forces, the effects are larger for the EC(A-H) force, except for CH_3^+. For the force $F_{H\perp}$, the effects of floating are seen in Table IV. In the fixed AO approximation, the AD force is neglected in the present minimal basis set. After the floating, however, it is largely improved for NH_3 and CH_3^+. For NH_3^+, the AD force is small even after the floating. This corresponds to a small distance Y of NH_3^+ shown in Figure 1. For NH_3, the effect of floating is also large for the EC(H-A) force. This is different from the previous results obtained by floating only the $1s_H$ AOs.[11,23] It seems to be due to the floating of the AOs belonging to the central atom. Further, we have confirmed that in the present calculations, a spurious "translational" force, which often appears in the H-F forces calculated from an approximate wave function, vanishes identically.

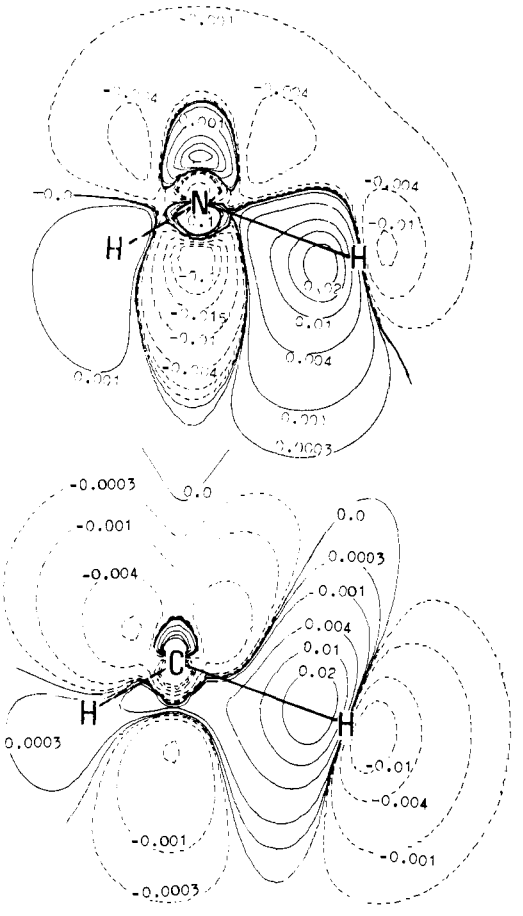

Figure 8. Effects of floating on the electron densities of NH_3 and CH_3^+ at $\theta = 15°$. The density difference is defined by eq A1 of the Appendix.

Figure 8 illustrates the effects of floating on the electron densities of NH_3 and CH_3^+ at $\theta = 15°$. It gives the contour map defined by

$$\Delta\rho = \rho(\text{float}) - \rho(\text{fixed}) \qquad \text{(A1)}$$

It is seen that the floating of the AOs accumulates the electron density in the A–H region. This accumulation results in an increase in the EC(A–H) force as shown in Table III. A difference between NH_3 and CH_3^+ is as follows. In NH_3 a larger amount of electron density is accumulated below the N–H axis, but in CH_3^+ it is accumulated above the C–H axis. This difference accounts for the different effects of the floating on the EC(H–A) forces of NH_3 and CH_3^+ (see Table IV). This difference also corresponds well to the similar difference in the bent bond nature depicted in the density maps shown in Figures 5 and 6. We further note that the order of magnitude of the floating effect is *not* small but very important in comparison with the order of the density reorganization due to the molecular formation from the separated atoms. This is especially so for NH_3 (comare the contour 0.02 au in Figure 8 with the contour 0.03 in Figure 5). In the regions of the central atoms, N and C, the effects of floating are more complicated than those in the A–H regions. For NH_3^+, the effect of floating on the density was similar but smaller by a factor of 2 than those for NH_3 and CH_3^+.

References and Notes

(1) H. Hellmann, "Einfuhrung in die Quantenchemie", Deuticke, Vienna, 1937, p 285; R. P. Feynman, *Phys. Rev.*, **56**, 340 (1939).
(2) An exhaustive review of the force concepts in chemistry has been given in (a) B. M. Deb, *Rev. Mod. Phys.*, **45**, 22 (1973), and will appear in (b) B. M. Deb, Ed., "The Force Concept in Chemistry", Van Nostrand-Reinhold, New York, N.Y., in press.
(3) (a) Parts 1–3: H. Nakatsuji, *J. Am. Chem. Soc.*, **95**, 345, 354, 2084 (1973). (b) Part 4: H. Nakatsuji and T. Koga, *ibid.*, **96**, 6000 (1974). (c) Parts 5 and 6; H. Nakatsuji, *ibid.*, **96**, 24,30 (1974).
(4) H. Nakatsuji and T. Koga in ref 2b, Chapter 4.
(5) R. F. W. Bader and A. K. Chandra, *Can. J. Chem.*, **46**, 953 (1968).
(6) (a) H. Nakatsuji, T. Kuwata, and A. Yoshida, *J. Am. Chem. Soc.*, **95**, 6894 (1973); (b) H. Nakatsuji, T. Koga, K. Kondo, and T. Yonezawa, *ibid.*, **100**, 1029 (1978).
(7) (a) B. M. Deb, *J. Am. Chem. Soc.*, **96**, 2030 (1974); B. M. Deb, P. N. Sen, and S. K. Bose, *ibid.*, **96**, 2044 (1974); (b) B. M. Deb, *J. Chem. Educ.*, **52**, 314 (1975); B. M. Deb, S. K. Bose, and P. N. Sen, *Indian J. Pure Appl. Phys.*, **14**, 444 (1976).
(8) R. F. W. Bader and H. J. T. Preston, *Can. J. Chem.*, **44**, 1131 (1966); J. L. Bills and R. L. Snow, *J. Am. Chem. Soc.*, **97**, 6340 (1975).
(9) R. J. Gillespie, "Molecular Geometry", Van Nostrand-Reinhold, Princeton, N.J., 1972.
(10) A. C. Hurley, *Proc. R. Soc. London, Ser. A*, **226**, 170, 179, 193 (1954); A. C. Hurley in "Molecular Orbitals in Chemistry, Physics, and Biology", P.-O. Löwdin and B. Pullman, Ed., Academic Press, New York, N.Y., 1964, p 161.
(11) (a) H. Nakatsuji, K. Matsuda, and T. Yonezawa, *Chem. Phys. Lett.*, **54**, 347 (1978); (b) *Bull. Chem. Soc. Jpn.*, **51**, 1315 (1978).
(12) We have chosen NH_3^+ instead of CH_3 since the SCF MOs based on the minimal STO-3G basis do not reproduce the planar geometry of CH_3 (see ref 18).
(13) An exception is the floating spherical Gaussian orbital (FSGO) wave function proposed by Frost. See A. A. Frost, *J. Chem. Phys.*, **47**, 3707, 3714 (1967).
(14) R. Moccia, *Theor. Chim. Acta*, **8**, 8 (1967); J. Gerratt and I. M. Mills, *J. Chem. Phys.*, **49**, 1719 (1968); R. Fletcher, *Mol. Phys.*, **19**, 55 (1970).
(15) (a) P. Pulay, *Mol. Phys.*, **17**, 197 (1969); (b) J. W. McIver, Jr., and A. Komornicki, *Chem. Phys. Lett.*, **10**, 303 (1971); (c) A. Komornicki, K. Ishida, K. Morokuma, R. Ditchfield, and M. Conrad, *ibid.*, **45**, 595 (1977).
(16) R. F. Stewart, *J. Chem. Phys.*, **52**, 431 (1970).
(17) W. J. Hehre, R. F. Stewart, and J. A. Pople, *J. Chem. Phys.*, **51**, 2657 (1969).
(18) W. A. Lathan, L. A. Curtiss, W. J. Hehre, J. B. Lisle, and J. A. Pople, *Prog. Phys. Org. Chem.*, **11**, 175 (1974).
(19) Though the floating distances of the inner $1s_A$ AOs were very small, their effects on the H–F forces were important.
(20) H. Shull and D. Ebbing, *J. Chem. Phys.*, **28**, 866 (1958); R. S. Baker, J. C. Giddings, and H. Eyring, *ibid.*, **23**, 344 (1955).
(21) S. Bell, *J. Chem. Phys.*, **68**, 3014 (1978).
(22) C. A. Coulson and B. M. Deb, *Int. J. Quantum Chem.*, **5**, 411 (1971).
(23) The explicit formulas of the partitioned forces are given in ref 4 and 6b. They are different slightly from those used in the previous floating calculations (ref 11).
(24) R. F. W. Bader and G. A. Jones, *Can. J. Chem.*, **39**, 1253 (1961); R. F. W. Bader, W. H. Henneker, and P. E. Cade, *J. Chem. Phys.*, **46**, 3341 (1967).
(25) C. Edmiston and K. Ruedenberg, *Rev. Mod. Phys.*, **35**, 457 (1963).
(26) The density of the free atom A, ρ_A, was calculated from the spherical configuration, $(1s)^2(2s)^2(2p_x)^{n/3}(2p_y)^{n/3}(2p_z)^{n/3}$, where $n = 3$ for NH_3, $n = 2$ for NH_3^+, and $n = 1$ for CH_3^+. The AO exponents used for the atoms A and H are the same as those used in molecular calculations. Note, however, that the force depends only on the total density ρ_{AH_3} and not on the reference density given in the brace of eq 7. The latter was introduced simply to make the maps more visual.
(27) T. Koga, H. Nakatsuji, and T. Yonezawa, *J. Am. Chem. Soc.*, submitted. See also T. Berlin, *J. Chem. Phys.*, **19**, 208 (1951).
(28) This was also seen with the use of the definition of the "bond paths". See, G. R. Runtz, R. F. W. Bader, and R. R. Messer, *Can. J. Chem.*, **55**, 3040 (1977).
(29) For example, see, P. Coppens, *Angew. Chem., Int. Ed. Engl.*, **16**, 32 (1977).
(30) A. Hartmann and F. L. Hirshfeld, *Acta Crystallogr.*, **20**, 80 (1966); T. Ito and T. Sakurai, *Acta Crystallogr., Sect. B*, **29**, 1594 (1973); D. A. Matthews and G. D. Stucky, *J. Am. Chem. Soc.*, **93**, 5954 (1971).
(31) C. A. Coulson and W. E. Moffitt, *Philos. Mag.*, **40**, 1 (1949).